Organic & Biomolecular Chemistry

Dynamic Article Links

Cite this: *Org. Biomol. Chem.*, 2011, **9**, 7547

www.rsc.org/obc

PAPER

Supramolecular chemistry of monochiral naphthalenediimides†

Tom W. Anderson,[a] G. Dan Pantoş*[a,b] and Jeremy K. M. Sanders*[a]

Received 12th July 2011, Accepted 15th August 2011
DOI: 10.1039/c1ob06147j

Three new *N*-desymmetrised naphthalenediimides (NDIs) are described, each containing one chiral and one achiral centre. The ability of such 'monochiral' NDIs to self-assemble into hydrogen-bonded helical nanotubes, to act as a sergeant in a 'sergeants-and-soldiers' system and to form a hexameric receptor for C_{70} was examined. Small differences at the achiral centre were found to have significant effects on the supramolecular properties of the NDI. All three new NDIs form nanotubes that bind C_{60}, but with different efficiencies, and one is a better sergeant than any of the dichiral NDIs investigated to date.

Introduction

Naphthalenediimides (NDIs), which are readily obtained from naphthalene dianhydride (NDA) and two amino acids *via* a microwave synthesis, self-assemble in chloroform or 1,1,2,2-tetrachloroethane (TCE) to form hydrogen-bonded helical nanotubes.[1,2] When two equivalents of a chiral amino acid are used, the resulting NDI possesses two identical chiral α-carbon centres, such as NDI **1** and its ester analogue **2**. The chirality of the amino acid determines the helical twist of the resulting nanotube: L-**1** gives P-helices, while D-**1** gives M-helices. A mixture of L-**1** and D-**1** self-sorts into two opposing helices. Majority-rules behaviour[3–9] is not observed in these systems because, unlike in other systems, the chiral centres are intimately involved in creating the helical structure. A pair of achiral amino acids may also be incorporated, producing an achiral NDI, such as **3** or **4** (Fig. 1). We previously reported that such achiral NDIs may be organised as soldiers by dichiral NDI sergeants in the so-called 'sergeants-and-soldiers effect',[10–19] leading to chiral amplification that is detectable using circular dichroism (CD) spectroscopy.[9]

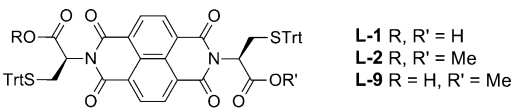

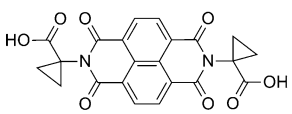

3

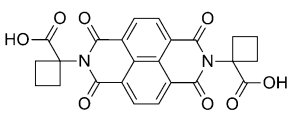

4

Fig. 1 The dichiral and achiral NDIs used in this work. Trt = trityl, $-CPh_3$.

The NDI nanotube is a receptor for numerous guests, most relevantly C_{60}.[20,21] This uptake can be observed using ^{13}C NMR, with the C_{60} carbon peak exhibiting a characteristic upfield shift due to shielding by the ring currents of the NDIs' aromatic cores and of neighbouring C_{60} molecules. The 'sergeants-and-soldiers' experiments revealed that hybrid nanotubes, made up of a mixture of chiral NDI L-**1** and achiral **3** or **4**, take up C_{60}, producing a slightly smaller upfield shift in the ^{13}C NMR. This was interpreted as the new achiral component introducing a subtle change in geometry or kinetic stability to the nanotube, which slightly reduces its ability to act as a C_{60} receptor.[9] In contrast, when C_{70} is added to a nanotube made up entirely of L-**1**, the nanotube is destroyed, the NDIs instead assembling into discrete hexameric C_{70}-receptor complexes with characteristic changes to the NDI ^1H NMR.[22] It does not appear that this receptor is formed by any of the achiral NDIs.[23]

The 'sergeants-and-soldiers' experiments demonstrated that small changes in the groups attached to the α-carbon of the achiral 'soldier' led to disproportionate changes in the behaviour of NDI analogues. NDI **3** was found to be the best 'soldier' achiral NDI (*i.e.* was most incorporated into L-**1** nanotubes), NDI **4** was an inferior but functional soldier and an NDI with two unconnected methyl groups at the α-carbon (derived from dimethylglycine, not pictured) showed no soldier activity at all. The most obvious differences between the NDIs were the bond angles and rigidity at the α-carbon, leading to a tentative explanation based on these factors.[9]

Having explored the very different behaviours of dichiral and achiral NDIs, we now report the synthesis and behaviour of 'monochiral' NDIs containing two different amino acids, one chiral and one achiral. These new building blocks help to answer questions regarding the formation of nanotubes and the ability of a single chiral centre to impose its preferred structure in a supramolecular assembly. The behaviour of monochiral NDIs towards C_{60} and C_{70} is also reported.

[a]*University Chemical Laboratory, University of Cambridge, Lensfield Rd., Cambridge, UK, CB2 1EW. E-mail: jkms@cam.ac.uk*
[b]*Department of Chemistry, University of Bath, Bath, UK, BA27 AY. E-mail: g.d.pantos@bath.ac.uk*

† Electronic supplementary information (ESI) available: CD and NMR data. See DOI: 10.1039/c1ob06147j

The dramatic changes in the sergeants-and-soldiers behaviour observed due to small changes in the nature of the achiral α-carbon on the achiral soldier suggested another aspect to this enquiry: if several different achiral amino acids were used to make several different monochiral NDIs (each sharing a common amino acid as the chiral component), would this produce analogously significant differences in their properties?

Results and discussion

The synthesis employed here follows a recently published procedure[24] using a lower microwave temperature for the first synthetic step. This method allows a monosubstitution of NDA by a chiral amino acid to form a naphthalene monoimide (NMI). The resulting NMI can then be worked up and used in lieu of NDA with one equivalent of the desired second amino acid, producing an *N*-desymmetrised NDI (Scheme 1). *S*-trityl-cysteine was the amino acid of choice in the first step, making NMI **5**, which in turn will lead to monochiral NDIs best suited for comparison with the dichiral NDI **1**.

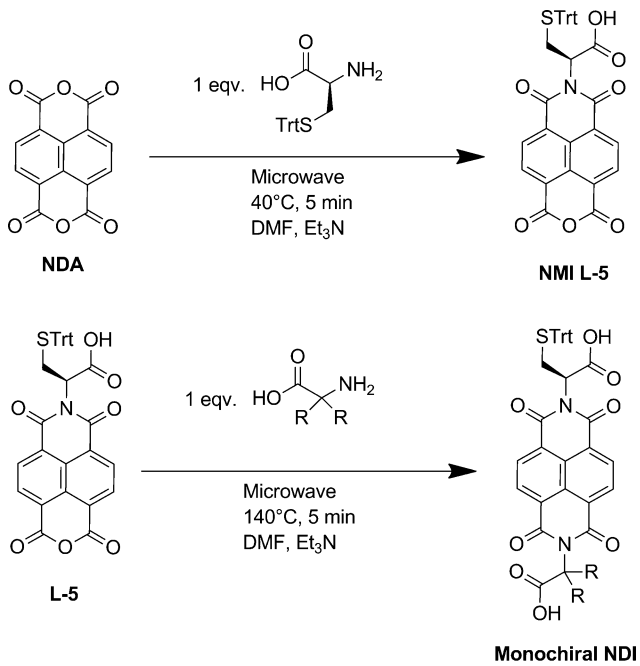

Scheme 1 The two-step synthesis of a monochiral NDI *via* NMI. R = two identical groups on an achiral amino acid.

Three monochiral NDIs were synthesised, as shown in Scheme 2. Two were derived from the same cyclopropyl- and cyclobutyl-derived amino acids as were used to synthesise the achiral NDIs **3** and **4**, while the third was glycine. A glycine-based achiral NDI had previously been synthesised and considered as a potential soldier for 'sergeants-and-soldiers' experiments, but proved insoluble in most organic solvents. These monochiral NDIs therefore represent both the investigation of two already studied achiral centres in a new molecular context and a way of looking at a centre that had been impossible to work with in an achiral NDI.

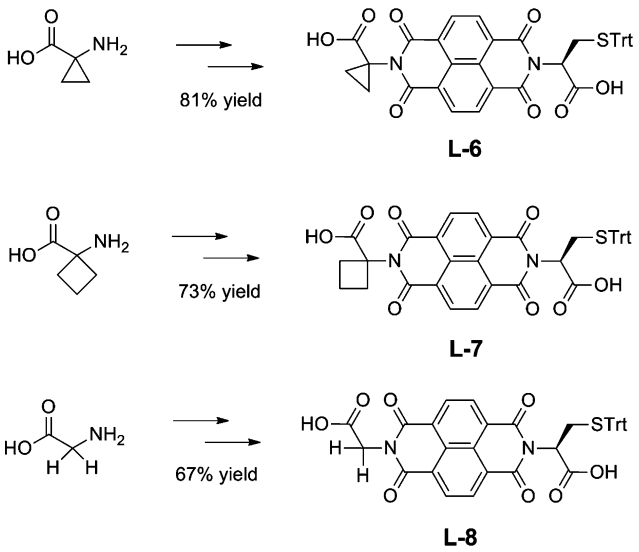

Scheme 2 Achiral amino acids and the resulting monochiral NDIs produced by their reaction with L-**5**. Yields given are for this final step only.

Nanotube formation

Equally concentrated solutions of monochiral NDIs L-**6**, L-**7** and L-**8** were prepared in TCE and their CD traces were compared to that of a solution of dichiral NDI L-**1** (Fig. 2). The three monochiral NDIs were found to produce CD signals of different intensities, which are indicative of different levels of nanotube formation.[25] The signal of NDI L-**6** is almost identical in strength to that of L-**1**, showing it forms nanotubes just as capably as its dichiral counterpart. However, the characteristic peak of the nanotube CD is slightly shifted to shorter wavelengths.

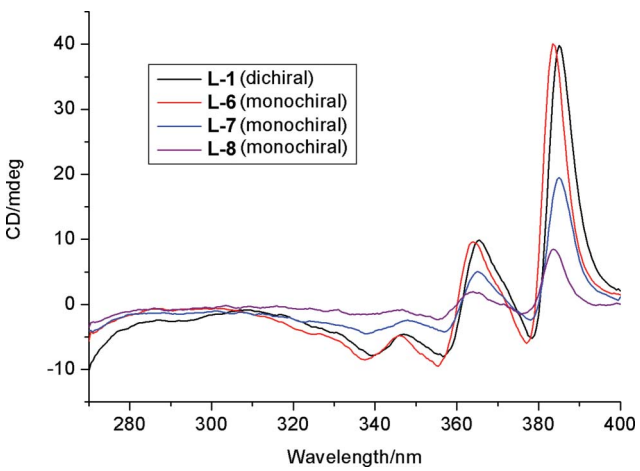

Fig. 2 CD traces of TCE solutions of monochiral NDIs L-**6**, L-**7** and L-**8** compared to that of dichiral L-**1**. Concentration of all solutions = 2.1 × 10^{-4} mol dm^{-3}.

This effect is also observed with 'sergeants-and-soldiers' mixtures of L-**1** and achiral **3**, suggesting that L-**6** can be thought of as an 'idealised' form of such a mixture, with the achiral **3** centres an integral part of each monomer.[9] The UV/vis absorbance spectra of L-**6** is also shifted relative to that of L-**1**, indicating the CD shift is due to the asymmetry of the NDI chromophore, rather

than changes in the interactions between adjacent molecules in the nanotube.[25]

The CD signals of NDIs L-**7** and L-**8** are progressively reduced in strength relative to L-**6**, indicating that nanotube formation is impaired. However, hydrogen-bonded assemblies are clearly present, as these signals collapse on the addition of 5% methanol (see Supporting Information†). While L-**7** unambiguously forms the nanotube, albeit not as well as L-**6**, the behaviour of L-**8** was less clear. The possibility existed that the hydrogen bonds formed through its glycyl end were too flexible to allow the formation of a nanotube and the small signal we observe is simply due to a dimer. In order to test this possibility, the CD spectrum of L-**8** was compared to that of an equally concentrated solution of NDI L-**9** (Fig. 1), a hybrid between L-**1** and L-**2** in which only one carboxylic acid is 'capped' with a methyl ester, so that it can only form dimers (Fig. 3).

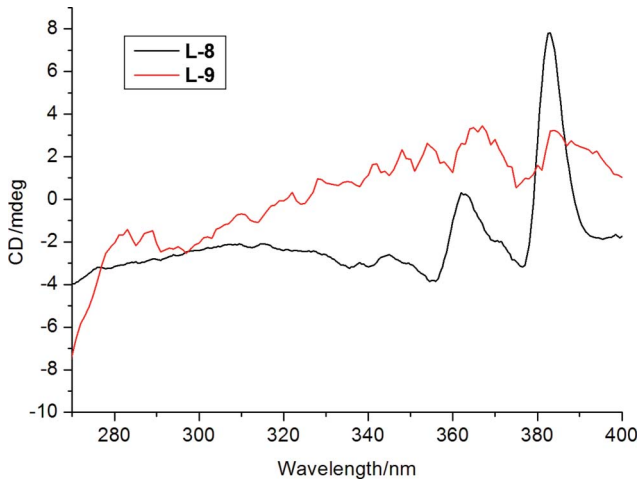

Fig. 3 A comparison of the CD traces of monochiral NDI L-**8** with the dichiral monoester L-**9** as solutions in TCE. The concentration of both solutions is 5.4×10^{-3} mol dm^{-3}.

The observed difference conclusively demonstrated that while the L-**8** CD signal is small, it definitely forms nanotubes rather than only dimers, and is therefore capable of hydrogen bonding through its glycyl ends; this observation is significant for the later experiments described below.

Evidence for hydrogen bonding

One issue with the previously published NDI nanotube work is that while everything points to these assemblies being held together by hydrogen bonds, the evidence for this is indirect. The hydrogen bonding of a nanotube made up of L-**1** cannot be observed using ^{1}H NMR, because although the hydrogen-bonded naphthyl protons should be in different chemical environments, the dynamic assembly and exchange of the NDIs to form the nanotube is sufficiently fast on the NMR chemical shift timescale that the naphthyl protons average to a single peak. However, the same is not true of monochiral NDI L-**6**, as can be seen by comparing the naphthyl region of the ^{1}H NMR spectra in 5% MeOD in $CDCl_3$ (in which nanotubes cannot form) and in pure $CDCl_3$ (in which they can). In the methanolic solution, the asymmetry of the L-**6** monomer means that the naphthyl protons are observed as two doublets coupling to one another. However, in the pure $CDCl_3$ solution they distinctively split further into four doublets, which is indicative of different chemical environments being imposed, presumably by hydrogen bonding (Fig. 4).[26]

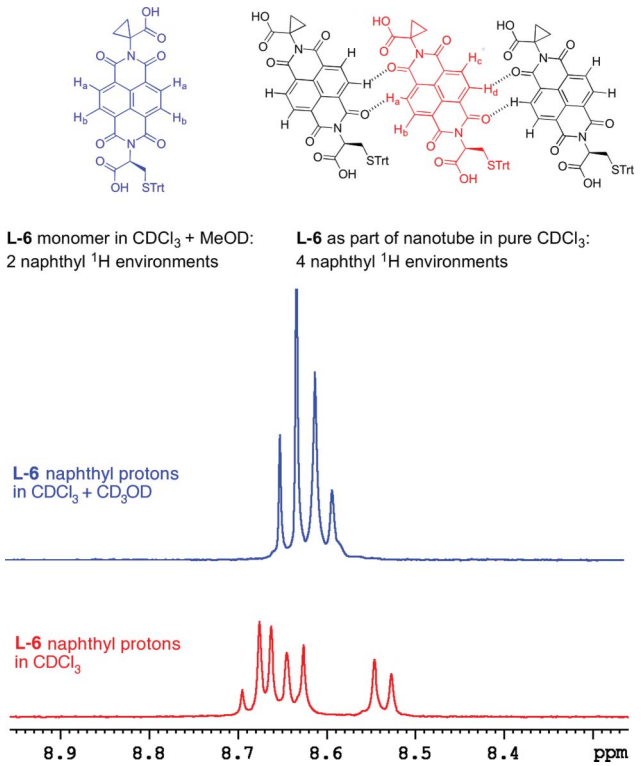

Fig. 4 A comparison of the naphthyl proton signals observed in the ^{1}H-NMR spectrum of NDI L-**6** under conditions in which the nanotube can and cannot form.

This result is significant as the first direct evidence of CH···O hydrogen bonding in the nanotube. However, it is also important because the fact that we can observe these different proton environments suggests that the assembly and disassembly of the L-**6** nanotube is significantly kinetically slower than that of the L-**1** nanotube.[27]

Uptake of C_{60}

Our previously published work showed that hybrid nanotubes made up of a 1 : 1 mixture of L-**1** sergeant and either **3** or **4** soldier were effective receptors for C_{60}, but slightly inferior to nanotubes composed only of L-**1**, and this difference seemed to be an intrinsic property of the hybrid nanotube.[9] If this interpretation was correct, we might expect nanotubes made up of L-**6** and L-**7** to be analogously poorer C_{60} receptors and perhaps comparable to the 1 : 1 mixture of L-**1** and the corresponding achiral NDI (as they contain the same proportions of chiral and achiral centres). ^{13}C NMR experiments carried out under the same conditions as previously showed that this prediction was broadly correct, although the monochiral nanotubes were actually slightly poorer receptors than the 1 : 1 mixtures (Fig. 5). The C_{60} peak represents a weighted average of the fast-exchanging C_{60} molecules inside the nanotube (shielded) and outside it (not shielded). Therefore, the more effective the nanotube is as a receptor, the more this peak is shifted upfield.

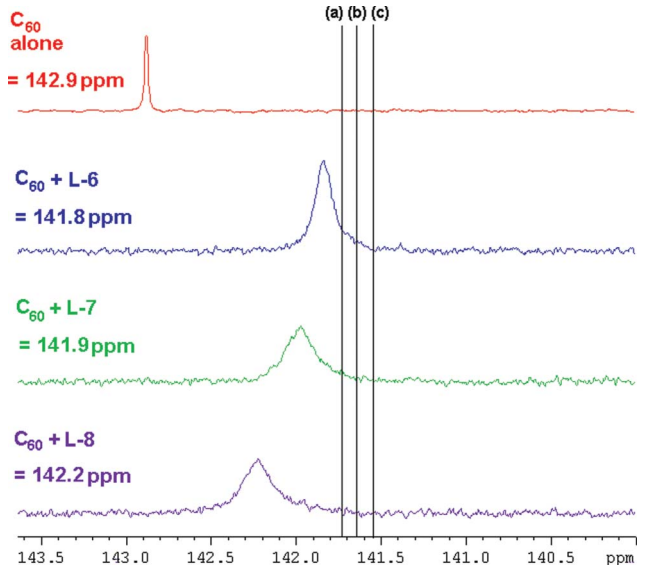

Fig. 5 ^{13}C NMR showing the C_{60} resonance and its shift when exposed to nanotubes made up of different NDIs in a solution of deuterated toluene. Vertical lines: (a) = C_{60} + a 1 : 1 mixture of L-**1** and **4**; (b) = C_{60} + a 1 : 1 mixture of L-**1** and **3**; (c) = C_{60} + L-**1**.[9] Each solution has the same molar quantity of NDI and C_{60}.

We had already hypothesised that the reduced ability of the hybrid nanotubes to act as C_{60} receptors was due to geometric differences in the way that the NDIs are arranged in the nanotube and this explanation can also be applied to the monochiral nanotubes. Clear confirmation that the geometry is different in the L-**6** nanotube to the L-**1** nanotube can be found by examination of the ^{1}H proton signal corresponding to the α proton (Fig. 6), which reveals major differences in the vicinal couplings to the β-protons in the two species.

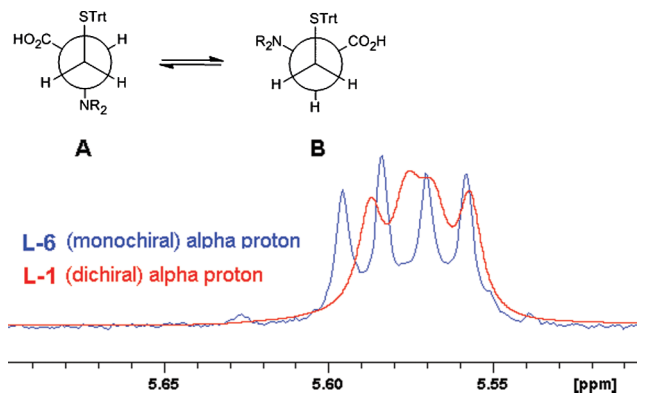

Fig. 6 ^{1}H NMR of the α-proton of NDIs L-**1** and L-**6** in deuterated TCE, together with Newman projections of the possible conformations of the α-carbon (back) and β-carbon (front). Note that the NMR spectra are not on the same vertical scale, as L-**1** has two α-protons per NDI whereas L-**6** only has one.

In both L-**1** and L-**6**, the α-proton couples to the two β-protons on the bridging β-carbon to the bulky –STrt group. These protons are diastereotopic, so the α-proton is split into a doublet of doublets. In L-**1**, the two coupling constants are similar: J_1 = 4.9 Hz, J_2 = 4.1 H, which are consistent with a conformation close to that labelled B in Fig. 6, in which both β-protons are gauche to the α-proton, and fits with the crystal structure obtained of L-**1** where all of the –STrt groups must point away from the nanotube to avoid steric clash.[2]

By contrast, the α-proton of L-**6** has J_1 = 9.8 Hz, J_2 = 5.1 Hz. This is consistent with conformation A, where the α-proton is gauche to one of the β-protons but anti to the other. Importantly, this effect is only observed under conditions when the nanotube can form: in the methanolic solutions in which it cannot assemble, L-**1** and L-**6** have almost identical α-proton coupling constants (see Supporting Information†).

This change in conformation can be rationalised based on the observation that L-**6** only has a bulky –STrt group at one end of the NDI. In an L-**1** nanotube there are possible conformations that are not adopted because they would place the –STrt group in a position where it can clash with another –STrt on an adjacent NDI, but in L-**6** the second –STrt is not present as the adjacent NDI presents its achiral end to the first NDI. This idea can also help us understand how individual molecules of NDI L-**6** are positioned in the nanotube (Fig. 7).

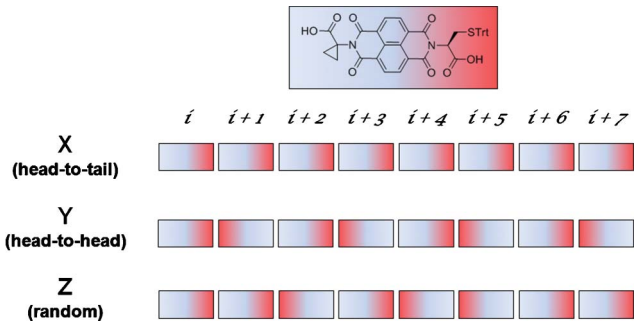

Fig. 7 Possible arrangements of NDI L-**6** in its nanotube (which, for clarity, is represented as a linear polymer). In the real helical nanotube, NDI *i* + 3 is immediately below NDI *i* as there are three NDIs per turn of the helix.

Case Z, a random arrangement, can be ruled out as it would not explain this change in conformation. Either of case X or Y is possible: it depends on whether the dominant steric clash between –STrt groups is between adjacent NDIs along the hydrogen-bonded chain (*e.g.* NDIs *i* and *i* + 1) or between NDIs immediately above or below each other in the helix (*e.g.* NDIs *i* and *i* + 3). The first would mean case X is correct as it places the chiral end of *i* next to the achiral end of *i* + 1, while the second would favour case **Y** as it places the chiral end of *i* immediately above the achiral end of *i* + 3 in the helix. Currently, we cannot assess which of these arrangements is the correct one.

Formation of the C_{70} receptor

A second question regarding the interaction with fullerenes is whether the new monochiral NDIs could also form the hexameric receptor for C_{70} observed with dichiral NDIs.[22] Initially these experiments were performed in deuterated TCE due to the fact that L-**8** has too low a solubility in chloroform. In the process of doing this work an unexpected solvent dependence for the formation of the C_{70} receptor was discovered: even NDI L-**1** does not form it in TCE or in toluene, chloroform being the only solvent in which this self-assembled receptor has yet been found to form. This was an intriguing discovery and the reasons behind it remain under study.

In chloroform, all three monochiral NDIs were found to form the C_{70} receptor in the presence of an excess of C_{70}. However, unlike L-**1**, they did not form the receptor exclusively, the equilibrium position between receptor and free monomer/nanotube being different for each monochiral NDI. This can be observed in the ^{1}H NMR of the naphthyl protons for each NDI, although integration of the peaks associated with the two species is approximate as they overlap. The most useful guide is the fact that, of the four doublets produced by the C_{70} receptor, one is much more downfield than the other three and separated from the peaks associated with the free NDI or nanotube, recalling from the earlier discussion that monochiral NDI nanotubes already produce multiple naphthyl peaks as opposed to a singlet in nanotubes made up of symmetrical NDIs like L-**1**. A second indicator is the α-proton shifting to a more downfield position. The change on the addition of an excess of C_{70} to L-**6** is shown in Fig. 8.

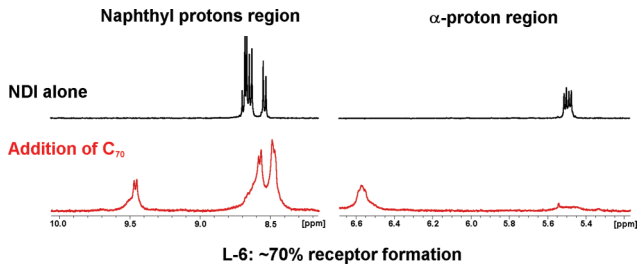

Fig. 8 ^{1}H NMR signals for the naphthyl and α-protons of NDIs L-**6** in deuterated chloroform, before (black) and after (red) the addition of C_{70}.

NDI L-**8**'s lower solubility in chloroform made the study of its NMR more problematic (see Supporting Information†), but it appears that less than 15% of the NDI forms the C_{70} receptor under these conditions. By contrast, integration shows that approximately 70% of NDI L-**6** and 30% of NDI L-**7** forms the receptor (see Supporting Information†). Perhaps significantly, this is the same trend across the three molecules as in their nanotubes' ability to act as a receptor for C_{60}.

An insight into the possible arrangements of monochiral NDIs around C_{70} was obtained from the observation that only one new α-proton signal is seen emerging as the C_{70} receptor is formed. This means that all of the chiral ends of the NDIs are in the same environment; with L-**1**, two α-proton signals are observed as those at the poles are in a different chemical environment to those at the equator. We cannot yet assign whether the monochirals' single α-proton signal is associated with the equatorial or axial position, but we can say that the arrangement of NDIs in the receptor is ordered rather than random (Fig. 9).

Monochiral NDIs as 'sergeants'

'Sergeants-and-soldiers' studies were carried out with monochiral NDIs L-**6**, L-**7** and L-**8** as potential sergeants, using the same protocol as previously reported.[9] This involves beginning with a cuvette 50% filled with soldier NDI solution and recording the CD after aliquots of 10% by volume of sergeant NDI solution (of the same concentration) are added until the cuvette is filled to a 1 : 1 mixture, giving a series of data points from 0–50% chiral solution. The protocol is then repeated with the two solutions swapped, giving data points from 50–100% chiral. A control data set is recorded by repeating these two experiment but replacing

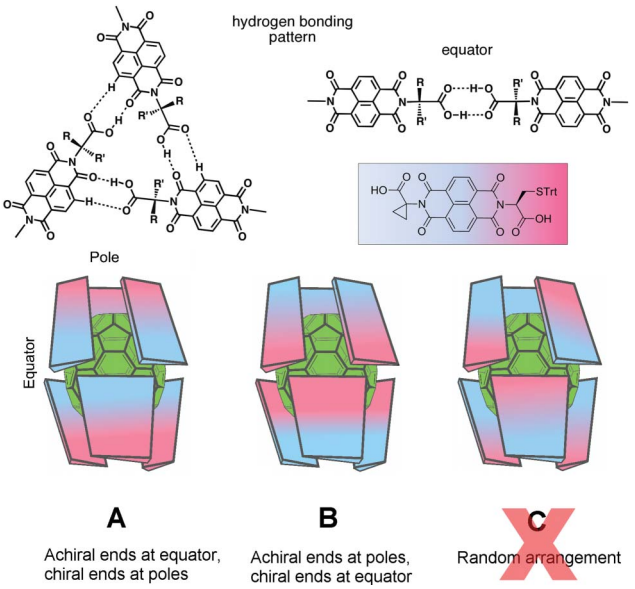

Fig. 9 The possible arrangements of NDI L-**6** in the C_{70} receptor and a schematic representation of the hydrogen bonding patterns at the pole[28] and equator of the hexameric capsule. The single α-proton signal means either A or B are possible, but C can be eliminated.

the soldier solution with one of NDI ester L-**2**, which cannot be incorporated into the nanotubes and provides a baseline by which the incorporation of soldiers may be judged. All four datasets are then plotted on the same graph, CD intensity against % chiral (*i.e.* % sergeant NDI) in the mixed solution.

For these experiments, the sergeant solution consisted of a solution of one of the monochiral NDIs. The results were surprising. While we might perhaps have expected monochiral NDIs to be inferior sergeants, the manner of their interaction with achiral **3** and **4** was unprecedented. NDIs L-**6** and L-**7** (L-**6**: Fig. 10; for L-**7**, see Supporting Information†) do act as sergeants, but only when soldiers **3** and **4** are present in higher concentrations than the sergeants. By halving the concentration of the starting solution of sergeant, a more familiar curve is obtained, but a comparison to L-**1** under the same conditions shows that the latter is still a superior sergeant (Fig. 10). The same effect is seen with **4** as the soldier (see Supporting Information†) save that, as previously reported, **4** is an inferior soldier to **3**. L-**7** also acts in this manner as the sergeant.

At present, we do not yet have a convincing theoretical explanation for this phenomenon. Fig. 2 demonstrates that NDIs L-**1** and L-**6** appear to form the nanotube equally readily, so any model to explain the difference in sergeant behaviour must take this into account.

NDI L-**8** has very different behaviour again. Far from a weaker and concentration-dependent sergeant activity, it is the strongest sergeant discovered for this system thus far, surpassing L-**1**. Because the CD signal for L-**8** is small compared to other monochiral NDIs, the protocol was slightly modified by averaging additional data sets and using a dilution method for the control data (See Supporting Information†) to minimise error, but the results (Fig. 11) are still comparable to other data sets based on equally concentrated solutions of sergeant and soldier.

This very large chiral amplification can be rationalised if we recall the idea that NDI L-**8** forms nanotubes less readily than

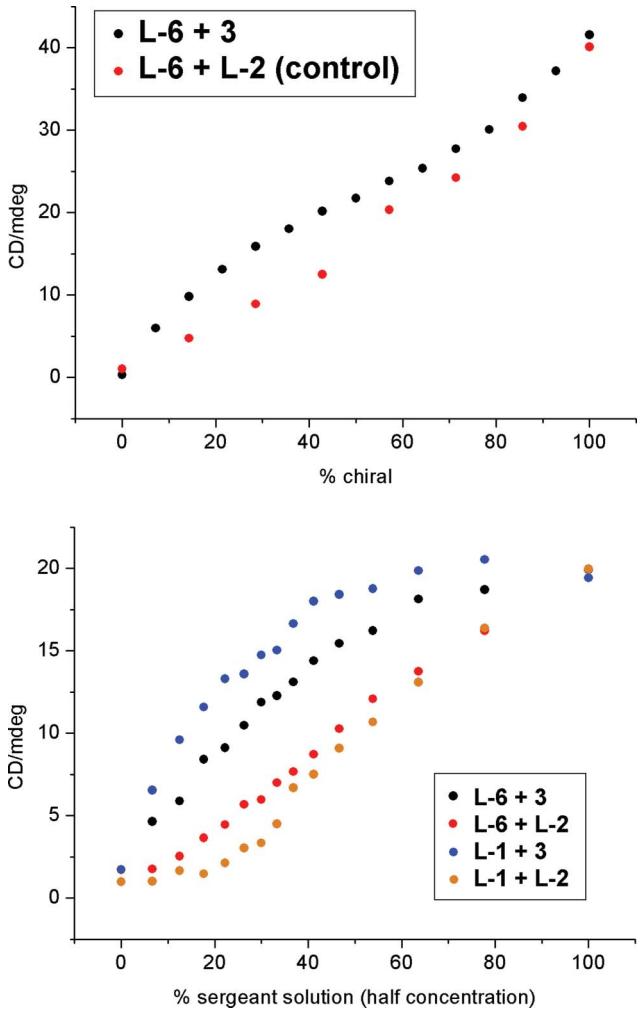

Fig. 10 The greater displacement above the control traces with inactive ester L-**2**, the more effective the 'sergeants-and-soldiers' behaviour. Using different mixtures of equally concentrated solutions of sergeant and soldier, L-**6** only acts as a sergeant when **3** is present in high concentration (low % chirality), which is made clearer when half-concentrated 'sergeant' solutions are used.

the other monochiral NDIs and this is presumably due to less favourable hydrogen bonding through its glycyl ends. NDI L-**8** also forms the least proportion of the C_{70} receptor, probably for the same reason. We can hypothesise that NDI **3** can act to bridge two molecules of L-**8** through their glycyl ends and allow the formation of longer oligomers than L-**8** alone can form. This explains why for ~60–90% L-**8**, the hybrid actually produces a stronger CD signal than L-**8** alone.

Conclusions

In this paper, we present a new set of NDI derivatives that helped us to explore the key role of chirality in the supramolecular nanotubes. All three new NDIs form nanotubes that bind C_{60}, but with different efficiencies, and one is a better sergeant than any of the dichiral NDIs investigated to date. Monochiral NDIs are not only interesting in their own right, but provide a tool to better understand the sergeants-and-soldiers interaction between dichiral and achiral NDIs. A geometric shift in the structure of the

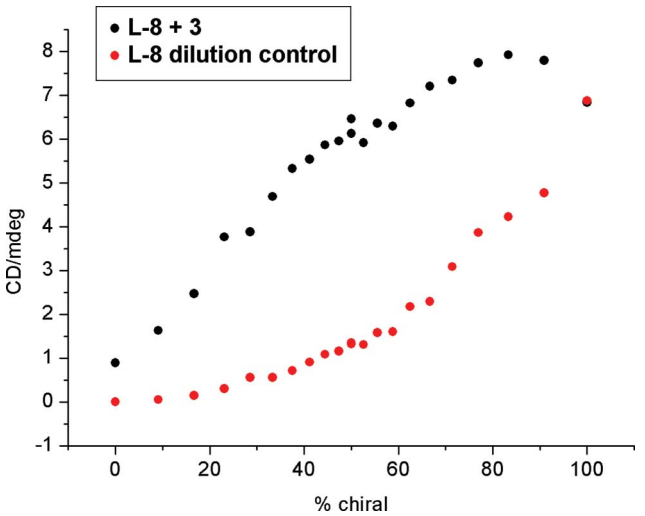

Fig. 11 The sergeants-and-soldiers data set for NDI L-**8** as the sergeant and **3** as the soldier. For the details of the control data set, see Supporting Information†.

NDI both helps us rationalise existing differences in the activity of nanotubes as C_{60} receptors and provide new ideas for future studies in this area. They have also provided us with more information about the nature of the C_{70} receptor. Monochiral NDIs allowed us to demonstrate how small changes in the molecular structure lead to markedly different behaviour in the macroscopic world.

Experimental

General methods

All solvents were of reagent grade quality (DMF, CH_3CN) or HPLC grade ($CHCl_3$) and purchased from standard suppliers. All starting materials were purchased from Aldrich and ChemImpex and used without further purification. Melting points were determined with a Gallenkamp apparatus and are uncorrected. NMR spectra were recorded on Bruker DRX 400 MHz or 500 MHz instruments. The NMR spectra were referenced to solvent and the spectroscopic solvents were purchased from Euriso-Top (C. E. Saclay) and Aldrich. All the spectra were recorded at 298 K. ^{1}H NMR data are reported as follows: chemical shift in ppm on the δ scale, integration, multiplicity (s: singlet, d: doublet, t: triplet, q: quartet, dd: doublet of doublets, bs: broad singlet, bt: broad triplet), coupling constants (Hz) and assignment. All high-resolution (HR) electrospray ionization mass spectra were recorded on a Waters LCT Premier XE instrument. The sonication was performed using a Bransonic 1210E tabletop ultrasonic cleaner. The microwave experiments were conducted using a CEM Discover™ Microwave Synthesizer. The CD analyses were performed on an Applied Photophysics Chirascan circular dichroism spectrometer. Compounds L-**1**, D-**1**, L-**2**, D-**2,3,4**, L-**5**, L-**9** and L-**9** were synthesized using previously reported methods.[1,2,24]

Synthesis of monochiral NDIs

NMI L-**5** (200 mg, 0.326 mmol) was dissolved in 5 mL DMF together with the corresponding achiral amino acid (0.326 mmol).

Et_3N (100 μL) was added. The suspension was sonicated until the mixture became homogenous. The reaction mixture was heated for 5 min at 140 ± 5 °C (direct flask temperature measurement) under microwave irradiation using a dedicated microwave system. The solvent was removed under reduced pressure and the reaction mixture was worked-up by being re-dissolved in EtOH (~5–10 mL) and poured into constantly stirred acidified water (5 mL 37% aqueous HCl in 500 mL water). This was allowed to stir at room temperature for a further 16 h, then filtered under suction. The product was collected as a yellow solid. The product was thoroughly dried under reduced pressure.

Characterisation data

L-**6** ((R)-1-(7-(1-carboxy-2-(tritylthio)ethyl)-1,3,6,8-tetraoxo-7,8-dihydrobenzo[lmn][3,8]phenanthrolin-2(1*H*,3*H*,6H)-yl)cyclopropanecarboxylic acid): Yield was 81% and further purification was not required. mp >300 °C; ^{1}H NMR (400 MHz, DMSO-*d*6) δ (ppm): 12.16 (bs, 1H) 12.93 (bs, 1H), 8.72 (s, 4H), 7.20 (m, 15H), 5.55 (dd, J_1 = 10.52, J_2 = 4.6, 1H), 3.12 (dd, J_1 = 12.76, J_2 = 4.8, 1H), 2.92 (dd, J_1 = 12.76, J_2 = 10.52, 1H), 1.81 (dd, J_1 = 9.8, J_2 = 4.4, 2H), 1.45 (dd, J_1 = 9.8, J_2 = 4.4, 2H); ^{13}C NMR (1H) (125 MHz, TCE-d_4) δ (ppm): 172.15, 169.18, 162.82, 161.95, 143.12, 129.03, 128.88, 128.07, 127.94, 126.97, 126.48, 126.21, 125.16, 66.47, 52.18, 34.82, 30.25, 18.38; HRMS (ESI+) calcd for: $C_{40}H_{28}N_2O_8S$ [M+H]$^+$ (*m*/*z*): 697.1639 found: 697.1582. Elemental analysis for 4 $C_{40}H_{28}N_2O_8S$·1 H_2O: calcd C, 68.51%; H, 4.10%; N, 3.99%; S, 4.57%; found: C, 68.53%; H, 4.11%; N, 4.00%; S, 4.58%.

L-**7** (R)-1-(7-(1-carboxy-2-(tritylthio)ethyl)-1,3,6,8-tetraoxo-7,8-dihydrobenzo[lmn][3,8]phenanthrolin-2(1*H*,3*H*,6H)-yl)cyclobutanecarboxylic acid): Yield was 73% and further purification was not required. mp >300 °C; ^{1}H NMR (400 MHz, $CDCl_3$) δ (ppm): 8.60 (s, 2H), 8.56 (s, 2H), 7.23 (m, 15H), 5.52 (dd, J_1 = 4.6, J_2 = 5.2, 1H), 3.18 (dd, J_1 = 12.1, J_2 = 5.2), 3.10 (dd, J_1 = 12.1, J_2 = 4.6, 1H), 2.69 (dd, J_1 = 12.4, J_2 = 8.9, 2H), 2.60 (dd, J_1 = 11.2, J_2 = 12.4, 2H), 2.45 (dd, J_1 = 9.6, J_2 = 8.9), 1.91 (dd, J_1 = 11.2, J_2 = 9.6); ^{13}C NMR (1H) (125 MHz, TCE-d_4) δ (ppm): 161.75, 161.51, 146.59, 130.75, 129.43, 128.28, 127.91, 126.79, 67.52, 62.99, 52.28, 36.46, 30.00, 16.78; HRMS (ESI+) calcd for: $C_{41}H_{30}N_2O_8S$ [M+H]$^+$ (*m*/*z*): 711.1796 found: 711.1783. Elemental analysis for 6 $C_{41}H_{30}N_2O_8S$·1 H_2O: calcd C, 68.99%; H, 4.28%; N, 3.92%; S, 4.49%, found C, 68.97%; H, 4.29%; N, 3.91%; S, 4.50%.

L-**8** ((R)-2-(7-(carboxymethyl)-1,3,6,8-tetraoxo-7,8-dihydrobenzo[lmn][3,8]phenanthrolin-2(1*H*,3*H*,6H)-yl)-3-(tritylthio)propanoic acid): Yield was 67% and required further purification: the product was recrystallised in hot chloroform/methanol (7 : 3 ratio) with the less soluble NDA starting material being removed *via* hot filtration. mp >300 °C; ^{1}H NMR (400 MHz, TCE-d_4) δ (ppm): 8.76 (d, J = 7.6, 2H), 8.70 (d, J = 7.6, 2H), 7.25 (m, 15H), 5.00 (dd, J_1 = 10.2, J_2 = 5.1), 3.28 (dd, J_1 = 6.8, J_2 = 5.1, 1H), 3.15 (dd, J_1 = 10.2, J_2 = 6.8, 1H), 2.9 (d, J = 28.1, 2H); ^{13}C NMR (1H) (125 MHz, TCE-d_4) δ (ppm): 161.94, 161.48, 143.88, 129.33, 128.28, 127.88, 127.19, 126.77, 126.21, 67.47, 56.71, 52.40, 29.62; HRMS (ESI+) calcd for: $C_{38}H_{26}N_2O_8S$ [M+H]$^+$ (*m*/*z*): 671.1488 found: 671.1479. Elemental analysis for 4 $C_{38}H_{26}N_2O_8S$·1 H_2O: calcd C, 67.60%; H, 3.96%; N, 4.15%; S, 4.75%; found C, 67.59%; H, 3.97%; N, 4.15%; S, 4.74%.

Acknowledgements

We thank Pembroke College, Cambridge, and the University of Bath (GDP) and EPSRC for financial support.

Notes and references

1 P. Pengo, G. D. Pantoş, S. Otto and J. K. M. Sanders, *J. Org. Chem.*, 2006, **71**, 7063.
2 G. D. Pantoş, P. Pengo and J. K. M. Sanders, *Angew. Chem., Int. Ed.*, 2007, **46**, 194.
3 M. M. Green, B. A. Garetz, B. Munoz, H. P. Chang, S. Hoke and R. G. Cooks, *J. Am. Chem. Soc.*, 1995, **117**, 4181.
4 J. van Gestel, A. R. A. Palmans, B. Titulaer, J. A. J. M. Vekemans and E. W. Meijer, *J. Am. Chem. Soc.*, 2005, **127**, 5490.
5 J. van Gestel, *Macromolecules*, 2004, **37**, 3894.
6 M. M. J. Smulders, P. J. M. Stals, T. Mes, T. F. Paffen, A. P. H. J. Schenning, A. R. A. Palmans and E. W. Meijer, *J. Am. Chem. Soc.*, 2010, **132**, 620.
7 A. R. A. Palmans and E. W. Meijer, *Angew. Chem., Int. Ed.*, 2007, **46**, 8948.
8 E. Yashima, K. Maeda, H. Iida, Y. Furusho and K. Nagai, *Chem. Rev.*, 2009, **109**, 6102.
9 T. W. Anderson, J. K. M. Sanders and G. D. Pantoş, *Org. Biomol. Chem.*, 2010, **8**, 4274.
10 M. M. Green, M. P. Reidy, R. J. Johnson, G. Darling, D. J. Oleary and G. Willson, *J. Am. Chem. Soc.*, 1989, **111**, 6452.
11 M. M. Green, N. C. Peterson, T. Sato, A. Teramoto, R. Cook and S. Lifson, *Science*, 1995, **268**, 1860.
12 C. Carlini, F. Ciardelli and P. Pino, *Makromol. Chem.*, 1968, **119**, 244.
13 A. R. A. Palmans, J. A. J. M. Vekemans, E. E. Havinga and E. W. Meijer, *Angew. Chem., Int. Ed. Engl.*, 1997, **36**, 2648.
14 L. Brunsveld, B. G. G. Lohmeijer, J. A. J. M. Vekemans and E. W. Meijer, *Chem. Commun.*, 2000, 2305.
15 R. B. Prince, L. Brunsveld, E. W. Meijer and J. S. Moore, *Angew. Chem., Int. Ed.*, 2000, **39**, 228.
16 R. B. Prince, J. S. Moore, L. Brunsveld and E. W. Meijer, *Chem.–Eur. J.*, 2001, **7**, 4150.
17 M. M. J. Smulders, A. P. H. J. Schenning and E. W. Meijer, *J. Am. Chem. Soc.*, 2008, **130**, 606.
18 S. J. George, Z. Tomovic, M. M. J. Smulders, T. F. A. de Greef, P. E. L. G. Leclere, E. W. Meijer and A. P. H. J. Schenning, *Angew. Chem., Int. Ed.*, 2007, **46**, 8206.
19 L. J. Prins, P. Timmerman and D. N. Reinhoudt, *J. Am. Chem. Soc.*, 2001, **123**, 10153.
20 G. D. Pantoş, J. L. Wietor and J. K. M. Sanders, *Angew. Chem., Int. Ed.*, 2007, **46**, 2238.
21 E. Tamanini, G. D. Pantoş and J. K. M. Sanders, *Chem.–Eur. J.*, 2010, **16**, 81.
22 J. L. Wietor, G. D. Pantoş and J. K. M. Sanders, *Angew. Chem., Int. Ed.*, 2008, **47**, 2689.
23 T. W. Anderson, PhD thesis, University of Cambridge, 2011.
24 K. Tambara, N. Ponnuswamy, G. Hennrich and G. D. Pantoş, *J. Org. Chem.*, 2011, **76**, 3338.
25 B. M. Bulheller, G. D. Pantoş, J. K. M. Sanders and J. D. Hirst, *Phys. Chem. Chem. Phys.*, 2009, **11**, 6060.
26 π–π interactions, which may lead to chiral aggregates that could have a similar set of naphthyl proton resonances, are unlikely to play a role in the self-assembly of the NDIs in chloroform, as the association constant between two molecules in this solvent is <1 M^{-1} (M. S. Cubberley and B. L. Iverson, *J. Am. Chem. Soc.*, 2001, **123**, 7560).
27 The nanotubes made up of monochiral L-**6** must cope with a constant 'mismatch penalty' from the fact that their components have both chiral and achiral centre-based carboxylic acid ends, which will slow their hydrogen-bonded assembly. The slower disassembly of L-**6** nanotubes may be due to the less sterically demanding packing of the smaller sidechains in L-**6** compared to L-**1**.
28 A similar hydrogen pattern has been previously observed in alanine phthalimide tapes: J. Li and Z.-P. Liang, *Acta Crystallogr. Sect. E*, 2006, **62**, o4915.